ELSEVIER

Thermochimica Acta 378 (2001) 35–44

thermochimica acta

www.elsevier.com/locate/tca

Catalysis by ATP synthase: mechanistic, kinetic and thermodynamic characteristics

Siddhartha Jain, Sunil Nath*

Department of Biochemical Engineering and Biotechnology, Indian Institute of Technology, Hauz Khas, New Delhi 110 016, India

Received 9 March 2001; accepted 2 June 2001

Abstract

Mechanistic, kinetic and thermodynamic aspects of ATP catalysis by ATP synthase have been determined and analyzed. Reversibility and irreversibility of catalysis in ATP synthase represent two contrasting modes of catalysis with important implications for the molecular mechanism of ATP synthesis. To shed light on these aspects, we have developed kinetic schemes for ATP synthesis and hydrolysis; analysis of these schemes reveals several novel features and provides new directions for further research. First, the ratio of bound $^{32}P_i$ to total bound ^{32}P can be expressed in terms of the rate constants of the elementary catalytic steps, which are characteristic properties of the system; therefore, results of classical cold chase/acid quench $^{32}P_i$ experiments interpreted in terms of an equilibrium distribution of bound substrate and product at the catalytic site can be explained by an irreversible mode of catalysis. Second, characterization of the mechanistic and kinetic properties reveals the absence of cooperativity in ATP synthase, and that product release precedes substrate binding. Third, ΔpH and $\Delta\psi$ are kinetically inequivalent in driving ATP synthesis, and $\Delta\mu_H$ is not the true driving force for ATP synthesis. Thermodynamic analysis of ATP synthesis reveals a dynamically electrogenic but overall electroneutral mode of ion transport across the membrane. The P/O ratio based on the torsional mechanism was obtained and was shown to explain the experimental observations of the past 50 years and to be in agreement with the thermodynamic calculations. Taken together, these findings necessitate a paradigm shift for understanding the molecular mechanism of ATP synthesis.

Keywords: ATP synthase; F_1; F_0; Kinetic model; Cooperativity; Inequivalence; Cold chase; Acid quench; Binding change mechanism; Torsional mechanism; Oxidative phosphorylation; Irreversibility; Competitive inhibition; Ion transport; Ion–protein interaction; Electroneutrality; P/O ratio; Thermodynamics; Dynamically electrogenic but overall electroneutral ion transport

1. Introduction

ATP is synthesized by the enzyme ATP synthase (or F_0F_1 ATPase) [1–5], which transforms energy from a transmembrane electrochemical gradient of protons [6–8] or, in some cases, Na^+ ions [9] into the chemical energy of ATP. This enzyme, the smallest known molecular machine, consists of two major parts [10,11]: a membrane-extrinsic, hydrophilic F_1 [12] containing three α-, three β-, and one copy each of γ-, δ-, and ε-subunits, and a membrane-embedded, hydrophobic F_0 [13,14] composed of one a-, two b-, and 12 c-subunits with the catalytic binding sites predominantly located in the β-subunits of F_1 at the α–β interface [1]. ATP synthesis takes place by conformational changes at the catalytic binding sites [15–18]. The exact mode of catalysis by ATP synthase remains an enigma, despite intensive research by several groups over the past several decades.

* Corresponding author. Fax: +91-11-686-8521.
E-mail address: sunath@dbeb.iitd.ernet.in (S. Nath).

0040-6031/01/$ – see front matter
PII: S0040-6031(01)00628-1

In order to explain ATP synthesis, various mechanisms have been proposed which can be classified into two broad categories based on the characteristics of catalytic steps: reversible catalysis [2,7,19–21] and irreversible catalysis [6,8,16,17,22–27]. The classical cold chase/acid quench $^{32}P_i$ experiments [19] are often cited as evidence for reversible catalysis by various groups. However, these experimental observations without exception can be explained logically and quantitatively by an irreversible mode of catalysis as shown by a detailed kinetic analysis in this work. From this analysis, we show that irreversible catalysis can also be used to explain ATP synthesis by ATP synthase. Further, kinetic analysis for irreversible catalysis by the F_0 and F_1 portions has been carried out and various mechanistic and kinetic implications have been discussed. We show the absence of cooperativity in ATP synthase, and kinetic inequivalence between the components of $\Delta\mu_H - \Delta\psi$ and ΔpH. Finally, we perform a detailed thermodynamic analysis of the torsional mechanism of ATP synthesis and contrast it with the binding change mechanism.

2. Experimental background

A commonly-accepted concept for ATP synthesis is that formation of enzyme-bound ATP from enzyme-bound ADP and P_i occurs reversibly with negligible change in free energy [1,19]. As an independent line of evidence in support of this concept, ATP hydrolysis experiments with mitochondrial F_1 in uni-site catalysis mode were performed, which led to the conclusion that subsequent to binding of substrate, an equilibrium is rapidly established in which the ratio of bound ATP to bound hydrolysis products ADP and P_i is 2, i.e. the equilibrium constant for reversible hydrolysis at the site is 0.5. [γ-^{32}P]ATP was used as substrate and the ratio of bound $^{32}P_i$/total bound ^{32}P, where total bound ^{32}P includes both bound $^{32}P_i$ and bound [γ-^{32}P]ATP, was measured at different concentrations of F_1 and [γ-^{32}P]ATP and at different incubation times of the reaction mixture and was observed to remain constant at one-third [19].

3. Kinetic analysis of ATP synthase

3.1. Kinetic scheme for ATP hydrolysis

A kinetic scheme based on a general sequence of events leading to ATP hydrolysis which considers irreversibility of the catalysis steps, as proposed recently by some researchers [6,8,16,17,22–27] was developed, as depicted in Fig. 1a. In this kinetic scheme, E represents the F_1-ATPase enzyme molecule, E.ADP the enzyme–ADP complex, E.ADP.P_i the enzyme–ADP–inorganic phosphate complex, and E.ATP the enzyme–ATP complex. K_1 and K_2 denote the dissociation constants of the corresponding elementary steps (Fig. 1a). The k_r denotes the rate constant for conversion of E.ATP to E.ADP.P_i, and k_r' the rate constant for conversion of E.ADP.P_i to E.ADP. The k_t stands for the constant of proportionality relating

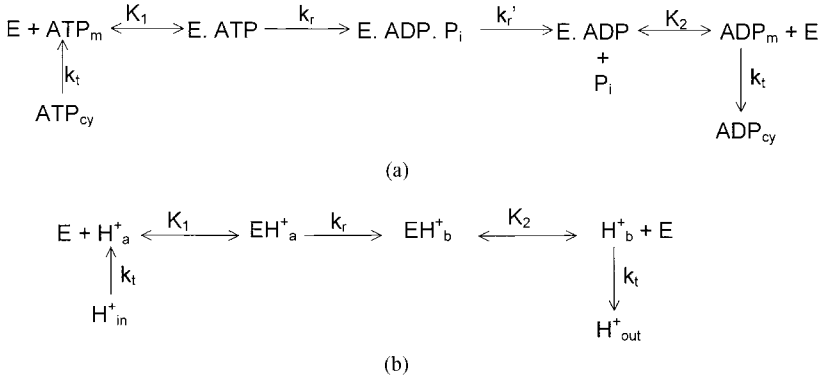

Fig. 1. (a) Kinetic scheme for ATP hydrolysis by F_1-ATPase. (b) Kinetic scheme based on the torsional mechanism of ATP synthesis by the F_0 portion of ATP synthase.

the rate of transport of adenine nucleotides by the adenine nucleotide transporter to the corresponding adenine nucleotide concentration gradients (Fig. 1a). The subscripts cy and m denote concentrations in the cytoplasm and mitochondrial matrix, respectively.

3.2. Prediction of $^{32}P_i/^{32}P$ ratio from the kinetic scheme

From the kinetic scheme, we define

$$f = \frac{\text{bound } ^{32}\text{P}_i}{\text{total bound } ^{32}\text{P}} = \frac{[\text{E.ADP.P}_i]}{[\text{E.ATP}] + [\text{E.ADP.P}_i]} \quad (1)$$

Because of the irreversibility of the catalysis steps, once ATP is bound to the F_1-ATPase, it has to get hydrolyzed to ADP and P_i. As E.ADP.P_i is an intermediate in ATP hydrolysis, quasi-steady state considerations imply that the rate of formation of E.ADP.P_i is equal to its rate of consumption, i.e.

$$v_{\text{hyd}} = k_{\text{r}}[\text{E.ATP}] = k'_{\text{r}}[\text{E.ADP.P}_i] \quad (2)$$

This implies that

$$[\text{E.ADP.P}_i] = [\text{E.ATP}]\left(\frac{k_{\text{r}}}{k'_{\text{r}}}\right) \quad (3)$$

Substituting Eq. (3) into Eq. (1) leads to

$$f = \frac{k_{\text{r}}}{k_{\text{r}} + k'_{\text{r}}} \quad (4)$$

Since $f = 0.33$ by experiment,

$$\frac{k_{\text{r}}}{k_{\text{r}} + k'_{\text{r}}} = 0.33$$

or

$$k'_{\text{r}} = 2k_{\text{r}} \quad (5)$$

3.3. Quasi-steady state constant for irreversible hydrolysis

From Eq. (4), we see that f is independent of both the concentrations of the enzyme and the substrate as well as the incubation time, as observed in the experiments. Since k_{r} and k'_{r} are rate constants, the fraction f is a characteristic property of the system. Similar to the equilibrium constant for reversible hydrolysis, we define a quasi-steady state constant for irreversible hydrolysis as K_{qss} = rate constant for formation of E.ADP.P_i/rate constant for consumption of

$$\text{E.ADP.P}_i = \frac{k_{\text{r}}}{k'_{\text{r}}} = 0.5 \quad (6)$$

The kinetic scheme analyzes the sequence of events occurring at a single site, which leads to the inference that the fraction f remains constant irrespective of the mode of catalysis, i.e. $f = 0.33$ for uni-, bi-, or tri-site catalysis. Thus, the kinetic scheme provides an alternative interpretation of the experimental observations and therefore, an irreversible mode of catalysis may also be employed to explain catalysis by F_1-ATPase.

4. Results and discussion

4.1. Kinetic model for the F_1 portion of ATP synthase

The possibility of irreversible catalysis in ATP synthesis has important mechanistic implications. Irreversibility in catalysis implies that catalysis in both F_0 and F_1 portions is irreversible. A mechanism that considers irreversibility is the torsional mechanism of ATP synthesis [6,8,16,17,22]. A general kinetic scheme was developed for ATP synthesis by the F_1 portion of ATP synthase based on the irreversibility of the P_i binding and enzyme-bound ATP synthesis elementary steps. Mathematical analysis of the kinetic scheme under steady state operating conditions leads to the following expression for the dependence of ATP synthesis on the adenine nucleotide concentrations

$$v_{\text{syn}} = V_{\max}\frac{\text{ADP}_{\text{cy}}}{\text{ADP}_{\text{cy}} + K_{\text{M}}(1 + \text{ATP}_{\text{cy}}/K_{\text{I}})} \quad (7)$$

where $V_{\max}$, K_{M}, and K_{I} are functions of the initial enzyme concentration and the rate and equilibrium constants of the elementary steps in the kinetic scheme [17].

4.2. Absence of site–site cooperativity in ATP synthase

The Michaellian nature of Eq. (7) indicates the absence of cooperativity among the catalytic sites of ATP synthase [16,17,28,29]. Although proposals involving cooperativity have been made for several decades [1,2,25,30–33], interactions among β-subunits have neither been detected by direct experiments

[33] nor shown to exist by theoretical considerations. Thus, the molecular basis of cooperativity still remains unelucidated [27]. The absence of any direct evidence for cooperativity in ATP synthase is explained, within the framework of the torsional mechanism, by the fact that site–site cooperativity does not exist [16].

4.3. Order of substrate binding and product release in F_1

Eq. (7) suggests the occurrence of competitive inhibition of ATP synthase by ATP as the inhibitor in the synthesis mode. This implies that the ATP competes with ADP, or the bound ATP changes the conformation of the site meant for ADP binding, thereby not allowing the ADP to bind to the catalytic site. Hence, unless product ATP is released, binding of substrate ADP is not possible. Thus, competitive inhibition imposes an order on binding and release events, i.e. product ATP release must precede substrate ADP binding. In contrast, mechanisms assuming reversible catalysis, such as the binding change mechanism [2,31,32], predict that substrate binding precedes product release.

4.4. Mechanistic implications in F_0 portion based on the kinetic model

A similar steady state analysis was carried out for the F_0 portion of ATP synthase using the kinetic scheme shown in Fig. 1b and the equation expressing the pH dependence of the rate of ATP synthesis was obtained as

$$v_{syn} = \frac{(k_s k_r E_0)H^+_{in}}{H^+_{in} + (K_1/K_2)H^+_{out} + (K_1 + k_r E_0/k_t)} \quad (8)$$

where k_s is a proportionality constant between the rate of rotation of the c-rotor and the rate of ATP synthesis. Eq. (8) can be rewritten in terms of the enzymological kinetic parameters V_{max}, K_M, and K_I [8]. This expression was compared to the experimental data [34] to determine the values of the enzymological kinetic parameters and the comparison between the simulated values and the experimental data for chloroplast ATP synthase for a single set of these parameters is depicted in Fig. 2. Eq. (8) suggests the presence of competitive inhibition by H^+_{out} as the inhibitor in the synthesis mode. This implies that H^+_{out} competes with H^+_{in}, or the H^+_b bound to its binding site on the c-rotor changes the conformation of the binding site for H^+_a on the c-rotor, thereby not allowing H^+_a to bind to its binding site. Hence, unless the binding site for H^+_b gets unprotonated, binding of H^+_a is not possible. Thus, an order is imposed on binding and release events in the F_0 portion of ATP synthase, i.e. during physiological steady state ATP synthesis, H^+_b unbinding and its

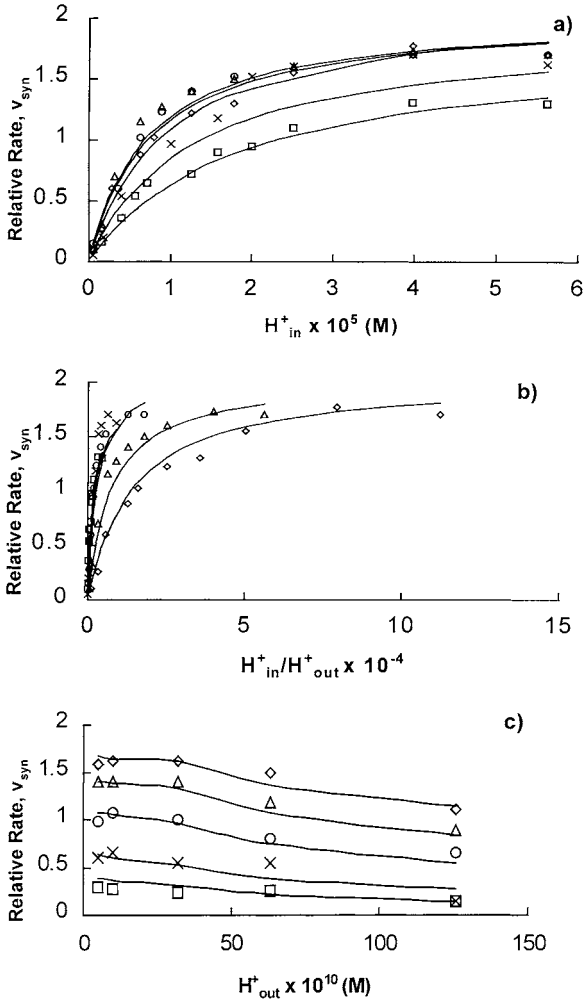

Fig. 2. Relative rates of ATP synthesis as a function of (a) H^+_{in}, (b) H^+_{in}/H^+_{out} and (c) H^+_{out} for chloroplast ATP synthase. Bold lines represent calculated rates using Eq. (8) obtained from our kinetic model and parameter values [8]. Points represent experimental data [34] — (a and b) pH_{out}: 9.3 (◇); 9.0 (△); 8.5 (○); 8.2 (×); 7.9 (□); (c) pH_{in}: 4.5 (◇); 4.8 (△); 5.1 (○); 5.5 (×); 5.8 (□).

subsequent release must precede H_a^+ binding. The rate constant for the rotation of the c-rotor, k_r (Fig. 1b) is a function of the electrical potential difference, $\Delta\psi$ [6,8,9,35] and since ΔpH and $\Delta\psi$ act at different elementary steps in the kinetic scheme based on our molecular mechanism of torque generation [6,8], the two components of the electrochemical potential difference, $\Delta\mu_H$ [36,37], are kinetically inequivalent. Further analysis using Eq. (8) by equating the rate of ATP synthesis due to an increase of ΔpH by one unit by increasing pH_{out} keeping pH_{in} constant with the rate of ATP synthesis by increasing $\Delta\psi$ (to a value $\Delta\psi'$), keeping ΔpH constant at its original value leads to the expression

$$\frac{k_r'}{k_r} = \frac{10[H_{in}^+/H_{out}^+ + (K_1/K_2) + (K_1/H_{out}^+)]}{10H_{in}^+/H_{out}^+ + (K_1/K_2) + (10K_1/H_{out}^+)} \quad (9)$$

By comparing the observed rate of ATP synthesis by chloroplast ATP synthase for ΔpH 4.4 at different $\Delta\psi$ [38] with Eq. (8), we observe that k_r shows a cubic dependence with respect to $\Delta\psi$ and the principal result for the rate of ATP synthesis in terms of ΔpH and $\Delta\psi$ works out to be

$$v_{syn} = \frac{57[1 + (\Delta\psi/42)^3]H_{in}^+}{H_{in}^+ + 900H_{out}^+ + (1.8 \times 10^{-6}) + 4.8 \times 10^{-6}[1 + (\Delta\psi/42)^3]} \quad (10)$$

where $\Delta\psi_{int}$ (=42 mV) is the value of the electrical potential difference due to the charge configuration and/or the diffusion of anions when there is no externally applied electrical potential. Eq. (10) can be used to simulate the rate of ATP synthesis as a function of ΔpH as well as $\Delta\psi$. The simulated rates of ATP synthesis as a function of pH_{in} at constant pH_{out} for various values of $\Delta\psi$, and as a function of $\Delta\psi$ for various values of pH_{in}, keeping pH_{out} constant are shown in Fig. 3. From the cubic dependence of k_r and k_r' in Eq. (9) on $\Delta\psi$ and $\Delta\psi'$, respectively, the values of $\Delta\psi'$ to match the rate of ATP synthesis obtained by increasing ΔpH by one unit can be calculated (Fig. 4). If ΔpH and $\Delta\psi$ had been kinetically equivalent driving forces, we would have obtained horizontal lines because the increase in $\Delta\psi$ required to match the rates would have remained constant irrespective of the value of ΔpH, as predicted by a model considering kinetic equivalence. However, a variation in $\Delta\psi'$ with pH_{in} and $\Delta\psi$ clearly indicates kinetic inequivalence of the two driving forces.

4.5. Thermodynamic analysis of molecular mechanisms for ATP synthesis

4.5.1. Energy transduction and ion transport in ATP synthase

During hydrolysis of ATP, the γ-phosphate bond of ATP is cleaved, resulting in the products ADP and P_i along with ∼35 kJ/mol of energy stored in the conformation of ATP. According to the binding change mechanism, energy is required only for release of synthesized ATP, but not for its synthesis [2,4,5,16]. This implies that E.ATP and E.ADP.P_i are isoenergetic. The binding change mechanism also conceives P_i binding to be spontaneous, which means that E.ADP.P_i and E.ADP are isoenergetic too. On the other hand, according to the torsional mechanism, all the elementary steps require energy, and the ion–protein interaction energy obtained from the ion gradients is used for synthesizing ATP, for P_i binding, and for straining the β–ε bond in order to enable ADP to bind. The energy to release preformed ATP from the tight catalytic site (β_{DP}) is provided by the formation of the β–ε ester linkage [6,16,17,22]. The comparison of energy requirement for ATP synthesis in the two mechanisms is depicted in Fig. 5, and the differences between the two mechanisms are highlighted. As per the torsional mechanism, since the system functions in a nonequilibrium steady state, and the mode of catalysis is irreversible, the Gibbs free energy cannot be employed to study the thermodynamic aspects of the energy transduction process in ATP synthase. Further, the binding change mechanism fails to explain the conversion and utilization of the total energy of the ion gradients (Fig. 5).

An extensive study is needed to understand energy coupling in the F_0 portion of ATP synthase. ATP synthesis has been demonstrated with the enzyme molecule isolated, purified, and reconstituted into liposomes, which do not contain any redox complexes [9,34,35,38]. Therefore, either $\Delta\psi$ is not created, or it

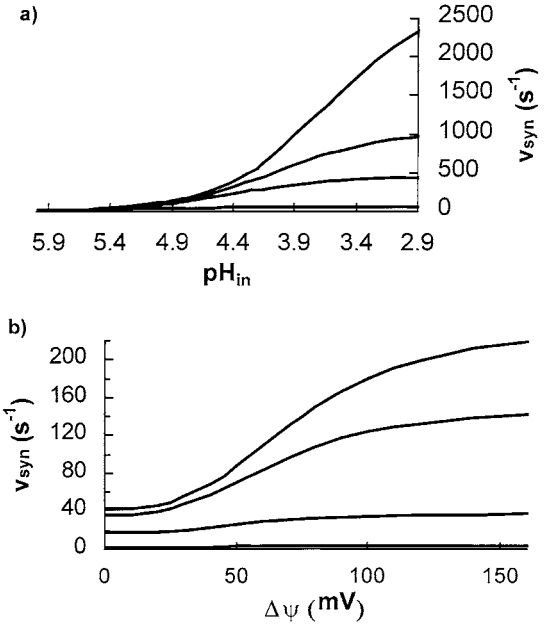

Fig. 3. Simulated rates of ATP synthesis catalyzed by chloroplast ATP synthase. (a) Rates of ATP synthesis as a function of pH_{in} at various values of $\Delta\psi$. The value of pH_{out} was kept constant at 9.3 and pH_{in} was changed from 2.9 to 5.9. The $\Delta\psi$ values for the curves (from bottom to top) were 0, 80, 108 and 152 mV, respectively. (b) Rates of ATP synthesis as a function of $\Delta\psi$ at various values of pH_{in}. The value of pH_{out} was 9.3 while $\Delta\psi$ was varied from 0 to 160 mV. The pH_{in} values for the curves (from bottom to top) were 6.6, 5.5, 4.9 and 4.7, respectively.

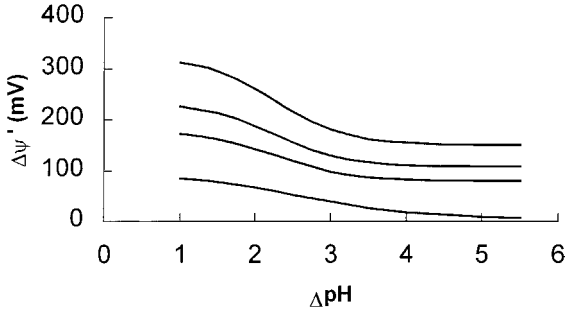

Fig. 4. Kinetic inequivalence of $\Delta\psi$ and ΔpH in driving ATP synthesis. The figure shows the electrical potential difference ($\Delta\psi'$) required to match the rate of ATP synthesis by chloroplast ATP synthase due to an increase in ΔpH of one unit (by increasing pH_{out} by one unit, keeping pH_{in} constant at 4.0). The curves represent different initial values of $\Delta\psi$ ($\Delta\psi_i$ from bottom to top) of 0, 80, 108 and 152 mV, respectively. The graph should be interpreted as follows. If ΔpH is increased from ΔpH_i to ΔpH_f keeping $\Delta\psi$ fixed at $\Delta\psi_i$, then, to match the rate due to this increase in ΔpH, the $\Delta\psi$ value needs to be increased to the value $\Delta\psi'$ corresponding to $\Delta pH = \Delta pH_i$ and the curve for which $\Delta\psi = \Delta\psi_i$.

is created in the vicinity of the ATP synthase enzyme complex, i.e. $\Delta\psi$ is localized. Since ΔpH supplies only half the energy requirement for ATP synthase, the rest has to be supplied by a locally present but independent source of $\Delta\psi$. One possible explanation suggested by several research groups is electroneutral transport of ions [39–42]; however, we postulate a dynamically electrogenic but overall electroneutral ion transport involving membrane permeable anions (such as succinate), and protons. In fact the importance of these membrane-permeable anions has been repeatedly emphasized [9,41–43]. In order to utilize the energy of the anion gradient, the anion flows along its concentration gradient through the membrane in the vicinity of the enzyme complex and creates a $\Delta\psi$ (negative inside) of -60 mV. This is followed by the transport of protons through the proton half-channel [6,8] along its concentration gradient. The proton binds to the essential Asp (or Glu) residue of the c-rotor resulting in a change in the overall $\Delta\psi$, $\Delta(\Delta\psi)$ of approximately 60 mV (30 mV due to ΔpH across the entry proton half-channel, and 30 mV due to change in $\Delta\psi$ upon proton binding to the Asp residue). The energy released in this step rotates the c-rotor by 15°. The incoming Asp residue releases its bound proton at the a–c interface, resulting in a $\Delta(\Delta\psi)$ of ~60 mV (30 mV due to ΔpH across the exit proton half-channel, and 30 mV due to change in $\Delta\psi$ upon proton unbinding from the Asp residue) and a consequent rotation of the c-rotor by 15°. During each 15° rotation of the c-rotor, the ion–protein interaction energy is transiently stored as twist in the helices of the 10 membrane-bound c-subunits. The simultaneous untwisting of the c-subunit helices drives the rotation of the ε-subunit and the bottom of the γ-subunit by 15°, and the ion–protein interaction energy is now stored as torsional energy in the γ-subunit. In this way, through cation binding *within* the electrostatic potential field created by the transport of anions, the enzyme is able to utilize the energy of both the delocalized ΔpH and the localized $\Delta\psi$.

When the K^+-valinomycin system is used, the H^+ moves in response to K^+ transport, and therefore, as the concentration of K^+-valinomycin is increased, H^+ transport increases and the rate of ATP synthesis correspondingly increases. However, when the K^+

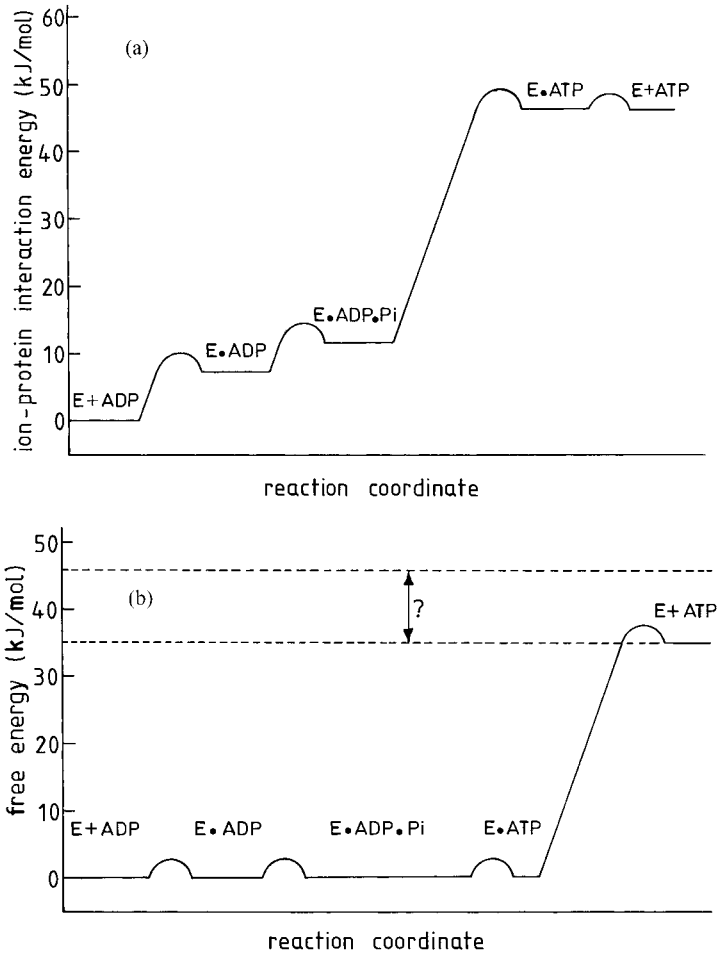

Fig. 5. Energy of the ion gradient as a function of the reaction coordinate during ATP synthesis by ATP synthase according to (a) torsional mechanism and (b) binding change mechanism.

transport attains a maximum limit upon saturation, the rate of ATP synthesis also becomes constant. This is in complete agreement with the experimental observations that the K^+/H^+ ratio increases with an increase in K^+ concentration and becomes constant at 4 for very high K^+ [39,40]. The dynamically electrogenic but overall electroneutral ion transport implies that if the transmembrane potential ($\Delta\psi$) is measured with nano/microelectrodes, the potential should be close to zero, as found by direct measurements on giant mitochondria [41,42]. The anion and the proton are transported back to the outside against the concentration gradients by the redox complexes, thereby storing the energy of oxidative phosphorylation as proton and anion gradients. In this context, we predict that Complex II in the respiratory chain (succinate ubiquinone oxidoreductase) transports anions against the concentration gradient and thus plays a key role in energy coupling. Hence, the proposed mechanism of dynamically electrogenic but overall electroneutral ion transport explains all the experimental observations on ATP catalysis.

4.5.2. Mechanistic P/O stoichiometry in oxidative phosphorylation

The question of mechanistic P/O stoichiometries has been the subject of extensive studies for over 50 years [44,45]; yet it remains an unresolved issue [46]. To address this aspect, we consider the dynamically

electrogenic but overall electroneutral ion transport for the complete process of oxidative phosphorylation in mitochondria. ATP synthesis is regulated by its demand for various cellular processes; when ATP^{4-} is required, it is transported out from the matrix to the cytoplasm along its concentration gradient. The electrical potential thus created drives ADP^{3-} along its concentration gradient to the mitochondrial matrix in exchange for ATP^{4-} by the adenine nucleotide transporter. The resulting unbalanced potential causes HPO_4^{2-} to move into the matrix, and the OH^- produced during ATP synthesis in the F_1 portion of ATP synthase [16,47] is driven out of the mitochondria in exchange for the HPO_4^{2-} by the HPO_4^{2-}/OH^- antiporter. The OH^- released per ATP produced is neutralized by a proton from the external medium, forming water. Thus, we need four protons to synthesize one molecule of ATP and one proton to neutralize the released OH^-, i.e. 5 H^+/ATP overall. In each cycle of oxidative phosphorylation, 12 protons are pumped out by the redox complexes with NADH-related substrates such as 3-hydroxybutyrate, and eight protons are transported from the matrix to the inner membrane against the concentration gradient with succinate as substrate. This implies that the mechanistic P/O ratio equals 12/5 (=2.4) and 8/5 (=1.6) for 3-hydroxybutyrate and succinate, respectively, for the *overall* oxidative phosphorylation process. This P/O ratio corresponds to the physiological steady state mode of operation. However, if only the *coupling* between the redox complexes and ATP synthase is considered, then the P/O ratio equals 12/4 (=3) and 8/4 (=2) for 3-hydroxybutyrate and succinate, respectively [23,24]. The experimentally observed P/O ratio will be lower than the mechanistic P/O due to the presence of proton leak through the membrane, as found [24,48,49]. It is worthwhile to note that if unsteady state experiments (pulse mode experiments) are carried out, the observed P/O ratios will depend on the time of incubation with 2.4 (complete neutralization of OH^-) and 3.0 (no neutralization of OH^-) as the theoretical lower and upper limits (without considering proton leaks). Thus, if the system is incubated for short durations (<1 min), all the OH^- released by the *population* of the ATP synthase molecules will not be neutralized by H^+, and the observed P/O ratio will be higher than that observed for steady state operation or for systems incubated for long durations (>2 min). According to the above analysis, the observed P/O (or J_P/J_O) should show a continuously decreasing trend with time during the state 3 to state 4 transition due to the progressive neutralization by protons of the hydroxyl ions released into the external medium. This is in complete agreement with classical experimental data recorded by Slater et al. for respiring mitochondria [48]. The consistently observed increase in the magnitude of the phosphorylation affinity (A_P) with time [48] during the state 3 to state 4 transition is explained by the progress of the system from the initial unsteady state non-optimal operation to its steady state optimal operation. The decrease of the P/O ratio with increase in (the magnitude) of A_P agrees with the nonequilibrium thermodynamic analysis of oxidative phosphorylation also [24]. In a systematic experimental investigation of mechanistic P/O ratios for mitochondrial oxidative phosphorylation [49], long incubation times of 4.5 min led to the lower values of the P/O stoichiometries of 2.27 for 3-hydroxybutyrate and 1.48 for succinate as substrate, as predicted by our analysis above. The same analysis can also be employed to explain the variation in observed P/O ratios with successive additions of substrate ADP to mitochondria [50]. In this study, for pyruvate + malate as substrates, P/O ratios as high as 3 and 2.6 were observed in the presence of EDTA and $MgCl_2$, respectively, for short incubation times of <60 s. The observed decrease in the P/O ratios (from 3.01 to 2.87 and from 2.58 to 2.51) occurs due to the unneutralized OH^- remaining in the medium from the previous incubat-ion. The longer incubation time during the second incubation (e.g. ~100 s instead of ~50 s for the EDTA case and ~75 s instead of ~50 s for $MgCl_2$) step led to partial neutralization of the OH^- remaining in the medium from the first and the second incubation steps, which was reflected in a slight increase (2.87–2.91 for EDTA) or a constant value (2.51 for $MgCl_2$) of the P/O ratio during the third incubation step.

One view to explain different P/O ratios for different classes of organisms is to consider variability in both the molecular mechanism as well as the stoichiometry of proton transport and ATP synthesis with the source of the enzyme [46]. However, considering our molecular mechanism and the energetics of the oxidative phosphorylation process, we believe that a universality in the mechanistic, kinetic and thermo-

dynamic characteristics of the system is operative. A possible explanation of the variations in the number of c-subunits and stoichiometries in some experiments [46] is the absence of the a-subunit during the formation of the c-ring. The a-subunit may be a critical determinant of the size of the c-ring and may well dictate the assembly of the individual c-subunits into the complete c-rotor.

Since, the phosphate potential ($x = A_P/A_O$) can be looked at as the fraction of the oxidative phosphorylation energy for synthesizing each ATP molecule, x can be taken as 1/3 and 1/2 for 3-hydroxybutyrate and succinate, respectively, which is in accordance with the experimental measurements for the state 3 phosphate potential in rat liver mitochondria [51,52]. Hence, for short incubation times, the mechanistic stoichiometry in the absence of proton leak, $Z = 3$ for 3-hydroxybutyrate, which corresponds to a degree of coupling, $q = 0.982$ [24,51] or $n = 5$ [51], which implies that the system optimizes output power, efficiency, and developed phosphate potential. On the other hand, for steady state operation or for long incubation times, $Z = 2.4$ for 3-hydroxybutyrate which corresponds to a $q = 0.986$ or $n = 6$, which implies that the system optimizes output power, efficiency, and developed phosphate potentials due to *protons as well as anions*. The occurrence of $n = 6$ for steady state operation, which is the physiological mode of operation, supports the dynamically electrogenic but overall electroneutral ion transport discussed in the previous section. Hence, knowledge of the underlying molecular mechanism of ion translocation permits the assessment of the final mechanistic stoichiometries for the oxidative phosphorylation process.

5. Summary

In summary, we have defined a quasi-steady state constant for ATP hydrolysis and shown it to be the ratio of the rate constants of the catalytic steps, and thereby a characteristic property of the system. Hence, the experimental observations can be explained by an irreversible mode of catalysis. Mathematical analysis of our proposed kinetic schemes based on irreversible catalysis enabled the study of the mechanistic and kinetic characteristics for both the F_0 and F_1 portions of ATP synthase in great detail. We find that there is no site–site cooperativity among catalytic sites [16,17,28,29] and that ATP release precedes ADP binding in the F_1 portion of ATP synthase. A *single* equation with a single set of enzymological kinetic parameters explains the experimentally observed pH dependence of the rate of ATP synthesis over the entire range. We have also simulated the rate of ATP synthesis as a function of ΔpH and $\Delta\psi$ and our general analysis predicts the rates of ATP synthesis by chloroplast ATP synthase under any set of operating conditions. Our analysis also shows that ΔpH and $\Delta\psi$ are kinetically inequivalent driving forces in ATP synthesis [6,8,35,38] and that $\Delta\mu_H$ does not drive ATP synthesis. Further, the change in $\Delta\psi$ needed to match the rate due to a change in ΔpH has been quantified. The apportioning of energy of the ion gradients among the elementary steps leading to ATP synthesis based on the torsional mechanism has been depicted and the differences vis-à-vis the binding change mechanism have been highlighted. Consideration of the ion transport across the membrane points to a dynamically electrogenic but overall electroneutral mode of transport. A detailed sequence of events for ion transport has been proposed and all the experimental observations in this context *without exception* have been explained. The mechanistic stoichiometry has been predicted based on the torsional mechanism and has been shown to explain the wealth of experimental data on the P/O ratios and be in agreement with the thermodynamics. These results point to the urgent need for a *paradigm shift* in the approach, thinking, analysis and interpretation to elucidate the molecular mechanism of ATP synthesis by ATP synthase.

Acknowledgements

This research has been generously supported by a special five-year (2001–2006) Golden Jubilee Research Project instituted on the occasion of the 50th anniversary of Indian independence by the Ministry of Science and Technology, Government of India.

References

[1] J. Weber, A.E. Senior, Biochim. Biophys. Acta 1319 (1997) 19.
[2] P.D. Boyer, Biochim. Biophys. Acta 1140 (1993) 215.

[3] T. Ramasarma, Curr. Sci. 74 (1998) 953.
[4] R.K. Nakamoto, C.J. Ketchum, M.K. Al-Shawi, Annu. Rev. Biophys. Biomol. Struct. 28 (1999) 205.
[5] W.S. Allison, Acc. Chem. Res. 31 (1998) 819.
[6] H. Rohatgi, A. Saha, S. Nath, Curr. Sci. 75 (1998) 716, Erratum: Curr. Sci. 78 (2000) 201.
[7] D.A. Cherepanov, A.Y. Mulkidjanian, W. Junge, FEBS Lett. 449 (1999) 1.
[8] S. Jain, S. Nath, FEBS Lett. 476 (2000) 113.
[9] G. Kaim, P. Dimroth, EMBO J. 18 (1999) 4118.
[10] J.P. Abrahams, A.G.W. Leslie, R. Lutter, J.E. Walker, Nature 370 (1994) 621.
[11] M.A. Bianchet, J. Hullihen, P.L. Pedersen, L.M. Amzel, Proc. Natl. Acad. Sci. U.S.A. 95 (1998) 11065.
[12] S. Wilkens, R.A. Capaldi, Nature 393 (1998) 29.
[13] R.H. Fillingame, W. Jiang, O.Y. Dmitriev, J. Exp. Biol. 203 (2000) 9.
[14] R.H. Fillingame, W. Jiang, O.Y. Dmitriev, P.C. Jones, Biochim. Biophys. Acta 1458 (2000) 387.
[15] H. Noji, R. Yasuda, M. Yoshida, K. Kinosita, Nature 386 (1997) 299.
[16] S. Nath, H. Rohatgi, A. Saha, Curr. Sci. 78 (2000) 23.
[17] S. Nath, S. Jain, Biochem. Biophys. Res. Commun. 272 (2000) 629.
[18] I. Ogilvie, R. Aggeler, R.A. Capaldi, J. Biol. Chem. 272 (1997) 16652.
[19] C. Grubmeyer, R.L. Cross, H.S. Penefsky, J. Biol. Chem. 257 (1982) 12092.
[20] H. Wang, G. Oster, Nature 396 (1998) 279.
[21] O. Pänke, B. Rumberg, Biochim. Biophys. Acta 1412 (1999) 118.
[22] S. Nath, H. Rohatgi, A. Saha, Curr. Sci. 77 (1999) 167.
[23] S. Nath, in: Proceedings of the 16th International Congress of Biochemistry and Molecular Biology, Vol. II, New Delhi, September 1994, p. 390.
[24] S. Nath, Pure Appl. Chem. 70 (1998) 639.
[25] J. Weber, A.E. Senior, J. Biol. Chem. 273 (1998) 33210.
[26] S. Löbau, J. Weber, A.E. Senior, Biochemistry 37 (1998) 10846.
[27] A.E. Senior, S. Nadanaciva, J. Weber, J. Exp. Biol. 203 (2000) 35.
[28] B.D. Reynafarje, P.L. Pedersen, J. Biol. Chem. 271 (1996) 32546.
[29] G. Berger, G. Girault, J.-L. Zimmermann, J. Bioenerg. Biomembr. 30 (1998) 543.
[30] P.D. Boyer, R.L. Cross, W. Momsen, Proc. Natl. Acad. Sci. U.S.A. 70 (1973) 2837.
[31] P.D. Boyer, Angew. Chem. Int. Ed. 37 (1998) 2296.
[32] Y. Zhou, T.M. Duncan, R.L. Cross, Proc. Natl. Acad. Sci. U.S.A. 94 (1997) 10583.
[33] N.P. Le, H. Omote, Y. Wada, M.K. Al-Shawi, R.K. Nakamoto, M. Futai, Biochemistry 39 (2000) 2778.
[34] F.P. Possmayer, P. Gräber, J. Biol. Chem. 269 (1994) 1896.
[35] G. Kaim, P. Dimroth, FEBS Lett. 434 (1998) 57.
[36] P. Mitchell, Nature 191 (1961) 144.
[37] P. Mitchell, Biol. Rev. 41 (1966) 445.
[38] S. Fischer, P. Gräber, FEBS Lett. 457 (1999) 327.
[39] S. Massari, G.F. Azzone, Eur. J. Biochem. 12 (1970) 301.
[40] G.F. Azzone, S. Massari, Eur. J. Biochem. 19 (1971) 97.
[41] H. Tedeschi, FEBS Lett. 59 (1975) 1.
[42] J.T. Tupper, H. Tedeschi, Science 166 (1969) 1539.
[43] A.T. Jagendorf, E. Uribe, Proc. Natl. Acad. Sci. U.S.A. 55 (1966) 170.
[44] S. Ochoa, J. Biol. Chem. 151 (1943) 493.
[45] L. Ernster, FASEB J. 7 (1993) 1520.
[46] S.J. Ferguson, Curr. Biol. 10 (2000) R804.
[47] H. Lodish, A. Berk, S.L. Zipursky, P. Matsudaira, D. Baltimore, J. Darnell, Molecular Cell Biology, 4th Edition, Freeman, New York, 2000, p. 647.
[48] E.C. Slater, J. Rosing, A. Mol, Biochim. Biophys. Acta 292 (1973) 534.
[49] P.C. Hinkle, M.A. Kumar, A. Resetar, D.L. Harris, Biochemistry 30 (1991) 3576.
[50] C.P. Lee, Q. Gu, Y. Xiong, R.A. Mitchell, L. Ernster, FASEB J. 10 (1996) 345.
[51] J.W. Stucki, Eur. J. Biochem. 109 (1980) 269.
[52] J.J. Lemasters, J. Biol. Chem. 259 (1984) 13123.